ORIGINAL RESEARCH ARTICLE

Effect of Annealing Temperature on the Electrochromic Properties of Electrochemically Oxidized Nickel

Meenu Maria Solly[1,3] · Neha Sharma[1,2] · Aarju Mathew Koshy[1] · Faiz Ali[1] · Sudha Arumugam[1,3] ·
Parasuraman Swaminathan[1,3] (iD)

Abstract

Electrochromic (EC) films are widely used in smart windows, automobile mirrors, and low-power displays due to their capability of reversibly changing color under an external potential. Transition metal oxides, due to their ability to switch between multiple oxidation states, are primarily used as EC films. They require low operating power and provide high coloration efficiency in EC applications. However, their thin-film fabrication through a low-cost and scalable process is still challenging. Here, nickel oxide (NiO) EC films have been synthesized by room-temperature electrochemical oxidation of Ni thin films. The Ni films were grown by electroless deposition and annealed at three different temperatures of 100°C, 200°C, and 300°C. The morphological, optoelectronic, and electrochemical properties of the films have been comparatively analyzed to obtain an optimized EC film. The NiO film annealed at 100°C exhibited superior properties with coloration and bleaching times of 1.8 s and 2.9 s, respectively, and a coloration efficiency of 20 cm^2/C. This annealed film is further used to fabricate a EC device with NiO and tungsten oxide (WO$_3$) as the electrode layers and a phosphoric acid-based gel as the electrolyte. The low-temperature deposition process used here can also be extended to flexible substrates.

Keywords Electroless deposition · electrochemical oxidation · nickel oxide · cyclic voltammetry · chronoamperometry

Introduction

The optoelectronic properties of transition metal oxides make them useful in a wide range of applications, such as photodetectors, gas sensors, displays, and solar cells.[1–5] The fast-switching speed and coloration efficiency of these metal oxides facilitate their use in a particular type of display device called an electrochromic (EC) device. Electrochromism is a phenomenon in which a persistent and reversible change in the optical absorption of a material occurs due to the insertion and extraction of electrons and ions.[6] EC devices are of considerable commercial and technological interest since they are non-scattering, stable, and retain their properties when switched back and forth between the colored and bleached states. They are preferred for transparent glazing or see-through applications, smart windows, displays, and rear view mirrors.[7,8] EC windows can be easily powered because of their low voltage requirement, which is helpful in energy conservation by reducing cooling/heating loads and by improving indoor comfort.[9] EC oxides are primarily of two types, cathodic coloring oxides (Ti-, Nb-, Mo-, and W-based oxides) which color upon ion insertion, and anodic oxides (Cr-, Mn-, Fe-, Ni-, and Co-based oxides) which color upon extraction of ions. WO$_3$, NiO, MoO$_3$, and V$_2$O$_5$ are the most commonly used EC metal oxides, of which NiO and WO$_3$ are widely studied.[10,11]

NiO has unique electrochemical and optoelectronic properties which make it popular in the EC industry. It possess high cyclic stability, high electrical conductivity, fast response time, well-defined and stable redox kinetics, and an efficient charge transfer mechanism.[12] Various deposition methods have been investigated in the preparation of

✉ Parasuraman Swaminathan
swamnthn@iitm.ac.in

1   Electronic Materials and Thin Films Lab Department of Metallurgical and Materials Engineering, Indian Institute of Technology Madras, Chennai 600036, India

2   Department of Electrical Engineering, AMOLED Research Centre, Indian Institute of Technology Madras, Chennai 600036, India

3   Centre of Excellence in Ceramics Technologies for Futuristic Mobility, Indian Institute of Technology Madras, Chennai 600036, India

NiO-based EC films, such as sputter coating,[13–15] electron beam evaporation,[16] thermal evaporation,[17] template-assisted hydrolysis,[18] sol–gel deposition,[19] aerosol-assisted chemical vapor deposition,[9] and hydrothermal synthesis.[20] Studies have been carried out by varying the deposition method and thickness to obtain the maximum coloration efficiency and fast response time. It has also been shown that a porous morphology in the NiO film enhances the EC performance by facilitating the fast intercalation/de-intercalation of ions.[9,21,22] Most of the current deposition techniques require high annealing or deposition temperatures. An alternate route is electroless nickel (Ni) deposition, which is an auto-catalytic process and can be carried out below 100°C.[23] However, to oxidize the deposited Ni, annealing above 500°C is usually required.[24] To avoid high-temperature annealing, room-temperature electrochemical oxidation can be carried out to convert Ni into NiO. This also converts the granular structure of the metallic film to a porous morphology which enhances the EC properties of the film.[25]

In this work, the electroless Ni deposition technique has been used to deposit Ni thin films, followed by electrochemical oxidation to produce NiO. The as-deposited Ni films are amorphous in nature[26] and we investigated the effect of annealing temperature of the Ni film on the EC properties. Uniform Ni deposition was carried out on fluorine-doped tin oxide (FTO) substrates and the film was annealed at 100°C, 200°C, and 300°C, followed by room-temperature electrochemical oxidation to convert the Ni to NiO. The surface, optical, and EC properties of the formed NiO films have been extensively characterized and, based on our results, the film annealed at 100°C was found to possess superior properties, including fast response time and high coloration efficiency. A prototype solid-state EC device was also fabricated using tungsten oxide (WO_3) and NiO as the electrodes and a phosphoric acid-based gel as the electrolyte. Given the low annealing temperature, the process developed here is also highly suitable for use with flexible substrates.

Materials and Methods

Materials

Nickel sulfate ($NiO_4.6H_2O$) and potassium hydroxide (KOH) were purchased from Merck Life Sciences (India), sodium citrate ($C_6H_5Na_3O_7.2H_2O$) and ammonium sulfate (($NH_4)_2SO_4$) were obtained from Avantor Performance Materials India, sodium hypophosphite monohydrate ($H_2NaO_2P.H_2O$) was purchased from Spectrochem (India), and polyvinyl alcohol (PVA; molecular weight 195,000) and orthophosphoric acid (H_3PO_4; 85% purity) were procured from Merck and Labchem, respectively. The solvents and

chemicals were used without further purification. FTO-coated glass slides (sheet resistance < 15 Ω/sq.) were purchased from Technistro India.

Preparation of NiO EC Film

The method followed in this work is adapted from a previous work in the group[25] and is described briefly below. The FTO glass slides were cleaned by sonication in acetone, ethanol, isopropyl alcohol, and de-ionized water for 7 min each using a Branson CPX2800H bath sonicator. The slides were then masked at the edges using a Kapton polyimide tape to create a 1 cm × 1 cm window at the center for Ni deposition. The glass surface was then activated by Au-Pd sputter-coating using a Polaron Series SC7640 high-resolution sputter coater (Quorum Technologies) operating at 1-kV DC output and 25-mA process current for 60 s. The chemical bath for electroless Ni deposition was prepared by adding 6 g each of nickel sulfate, ammonium sulfate, and sodium citrate, and 2.73 g of sodium hypophosphite in 200 ml of de-ionized water. The solution was stirred at room temperature using an IKA C-MAG HS-7 stirrer until the chemicals were completely dissolved.[26] The pH of the bath was 5.6. The bath was then heated to 60°C in an IKA C-MAG HS-7 digital hot plate with an attached thermocouple and electroless deposition was carried out for 30 s. The samples were further annealed in an oven at 100°C for 60 min to evaporate the solvents and moisture, and the obtained film was labeled EN-100. Other samples were further annealed at 200°C and 300°C for 60 min and denoted as EN-200 and EN-300, respectively. These Ni films were then electrochemically oxidized at room temperature to convert them into NiO.[25]

Fabrication of NiO-Based EC Device

Of the films annealed at different temperatures, the EN-100 film was used to fabricate an EC device by incorporating a 150-nm-thick WO_3 film (2.5 cm × 2 cm) as the anode. The WO_3 film was DC magnetron-sputtered at room temperature on an FTO substrate from a pure tungsten target at 100-W power in an argon and oxygen atmosphere, with flow rates of 20 and 25 standard cubic centimeters per minute, respectively. The fabrication and electrochromic properties of this WO_3 film were detailed in our previous work.[27] A PVA/H_3PO_4 polymer gel was used as the electrolyte for this solid-state EC device. First, a PVA gel was prepared by mixing 1 g of PVA in 10 mL distilled water using a REMI 2MLH stirrer at 80 ± 2°C for 2 h. H_3PO_4 was then added to this viscous solution to obtain the electrolyte solution of 1.86 M concentration, which was next coated over both the NiO and WO_3 films via spin coating. These electrolyte-coated films were then sandwiched and heated at 60°C for 30 min. The electrical connections were made using copper tape.

Characterization

The surface characterization of the as-deposited and oxidized samples was carried out using a Apreo S field-emission scanning electron microscope (FESEM) with an energy dispersive spectroscopy (EDS) setup. The thickness of the films were measured using a Nanomap 1000WLI (AEP Technology) optical profilometer. The optical transmittance spectra were obtained using a JASCO V-660 UV–Vis spectrophotometer. Cyclic voltammetry (CV) and chronoamperometry (CA) studies of the samples were carried out using a Biologic SP-150 and a Metrohm Autolab potentiostat, respectively. A three-electrode system in 1-M KOH solution with the Ni film on FTO as the working electrode, Pt mesh as the counter electrode, and Ag/AgCl in 3-M KCl electrolyte as the reference electrode was run for 420 cycles in the potential window − 0.2 V to 1 V at a scan rate of 20 mV/s to convert the Ni film to NiO film. For the CV measurements, a linear potential sweep was applied from − 0.2 V to 1 V for 10 cycles to observe the cyclic stability of the film. CA was performed at a potential of − 0.2 V and 1 V to study the switching behavior of the film from the colored to the bleached state and vice versa.

Results and Discussion

Morphological Studies

Figure 1a, b, and c shows SEM images of the Ni films annealed at different temperatures, while Fig. 1d, e, and f shows the same films after electrochemical oxidation. It can be seen that there are no visible changes in the microstructure of the films with the increasing annealing temperature, except for a slight increase in the average grain size. During electroless deposition, the Ni grains are deposited on the substrate in an island growth mode[23] and, as more material is deposited, these islands grow and meet to form a continuous layer on the substrate. For the deposition conditions used in this work, a film of thickness approximately 47 nm (as measured using the optical profiler) was obtained. The thickness was optimized based on our previous work on EN films.[25] Thinner films did not show a stable and repeatable EC behavior while thicker films had a lower optical transmittance, both in the colored and bleached states. From Fig. 1, it can be seen that the granular morphology of the Ni film is changed to a porous nanoflake morphology upon electrochemical oxidation. A similar morphology change was also observed for the electroless Ni films, without any post-annealing treatment.[25] The morphology change occurs because, during the oxidation and reduction cycles, OH⁻ ions are, respectively, inserted and extracted from the Ni film.[28]
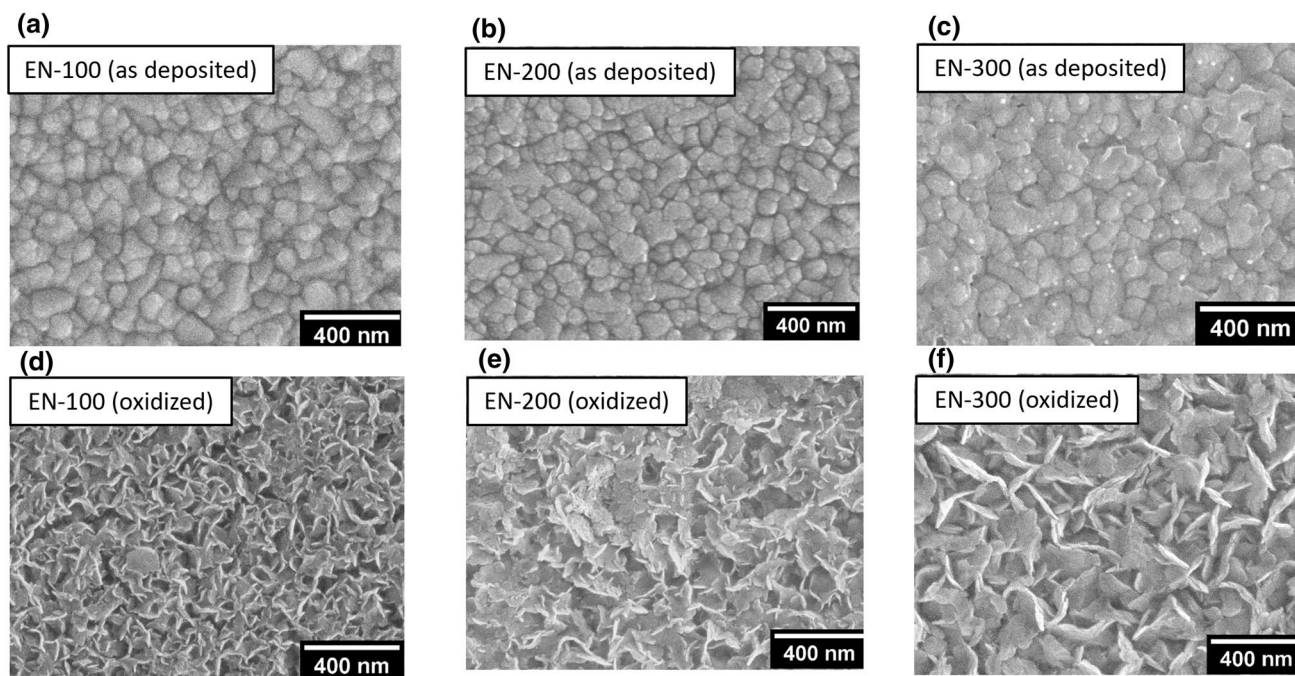

Fig. 1 Scanning electron microscope images of the as-deposited and oxidized films: (a, b, and c) the deposited EN-100, EN-200, and EN-300, respectively; (d, e, and f) the electrochemically oxidized EN-100, EN-200, and EN-30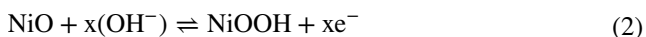0, respectively. With electrochemical oxidation, the granular morphology transforms into a porous nanoflake morphology which helps in the insertion/extraction of the ions and improves the EC film. The film annealed at 100°C has the smallest nanoflake size and hence shows the best EC properties.

The rough morphology of the oxidized samples enhances the EC properties of the film, since the increased surface area improves the ion insertion kinetics in the film.[29,30] It can be observed qualitatively from the SEM images that the size of the nanoflakes increases with the annealing temperature. The smaller flakes in EN-100 make it more porous and hence enhance the EC behavior due to the enhanced surface area compared to the films annealed at higher temperatures.

Cyclic Voltammetry Analysis

The Ni films were subjected to electrochemical oxidation to convert them into NiO which is optically transparent. CV was performed on the NiO films to study their electrochemical properties. Figure 2 compares ten CV cycles for the EN100, EN-200, and EN-300 films.

The EC behavior of NiO is attributed to the transition between the Ni^{2+} and Ni^{3+} oxidation states.[31] Coloration occurs when the transparent NiO and $Ni(OH)^-$ are oxidized to NiOOH and bleaching occurs when the NiOOH is reduced. In the anodic scan, the intercalation of OH^- ions into the transparent NiO film results in the oxidation of Ni^{2+} to Ni^{3+}, which changes the color of the film to dark brown. During the reverse cathodic scan, the de-intercalation of OH^- ions from the colored NiOOH film results in the reduction of Ni^{3+} back into Ni^{2+}, which bleaches the film back to the transparent state. The whole process can be summarized using:[32–35:]

$$NiO + H_2O \rightleftharpoons Ni(OH)_2 \tag{1}$$

$$NiO + x(OH^-) \rightleftharpoons NiOOH + xe^- \tag{2}$$

$$Ni(OH)_2 + x(OH^-) \rightleftharpoons NiOOH + H_2O + xe^- \tag{3}$$

All three samples (EN-100, EN-200, and EN-300) were cycled ten times to observe the cyclic stability and the data are shown in Fig. 2. The diffusion coefficient of the OH^- ions within the film has been calculated from the Randles–Sevcik relationship[36–38:]

$$i_p = 2.75 \times 10^5 \times n^{2/3} \times D^{1/2} \times C_0 \times \upsilon^{1/2} \tag{4}$$

where I_p is the anodic peak current density, n is the number of electrons, D is the diffusion coefficient, C_0 is the number of active ions in the electrolyte, and υ is the scan rate. The calculated diffusion coefficient for the samples are 8.6×10^{-12} cm^2/s, 8.7×10^{-12} cm^2/s, and 8.6×10^{-12} cm^2/s for the samples EN-100, EN-200, and EN-300, respectively. These values are consistent with values reported in the literature.[36,39] Typically, the higher the value of D, the faster the EC reaction, since movement of ions is easier. The comparable values of D for all three films indicate that the movement of ions within the NiO is not affected by the annealing conditions prior to oxidation. However, when comparing the CV curves from Fig. 2, it can be seen that the curve for EN-300 is shifted to slightly higher voltages compared to EN-100 and EN-200. This leads to slightly longer switching times. Similarly, for EN-200, the cyclic stability is lower since the curve for the tenth cycle is shifted by approximately 5% to the left compared to the first cycle. This sort of shift is not observed for EN-100 and EN-300.

Chronoamperometry Studies

For an EC device, switching (response) time is an important factor to determine its efficiency. Switching time is the time taken by the device to reach 90% of the complete response. To obtain the switching time between the colored and bleached states of the NiO films, CA studies were carried out. A potential of 1 V (for coloration) and − 0.2 V (for bleaching) were applied for 30 s each for a total time of 300 s, and the resulting graphs are shown in Fig. 3 for the films annealed at the three different temperatures.
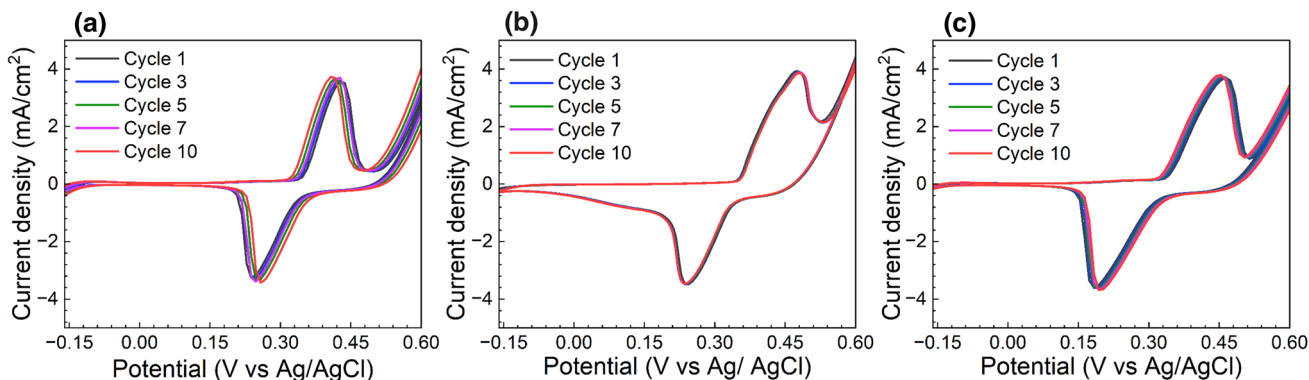

Fig. 2 Ten cyclic voltammograms recorded in the 1-M KOH electrolyte at a scan rate of 20 mV/s for (a) EN-100, (b) EN-200, and (c) EN-300; the data clearly establish the cyclic stability of the films.

The response times, t_c (coloration time) and t_b (bleaching time), for each film were calculated from the CA curves and shown in Table I. The EN-100 film has the shortest response time for coloration compared to the other two samples. This is because a higher annealing temperature makes the film more dense, decreasing the rate of ion intercalation and de-intercalation in the film.[36] The coloration and bleaching times for EN-100 and EN-200 are constant throughout the cycles, giving a sharp switch between the states, whereas it was found to vary in the case of EN-300.

Electrochromic Properties

The as-deposited Ni films appear gray in color and, upon electrochemical oxidation, turn transparent due to the formation of NiO. During voltage cycling, the transparent films turn dark brown on oxidation and back to transparent/bleached state on reduction (Fig. 4). UV-Vis transmittance spectra were obtained for the as-deposited, colored, and bleached states for all three samples, i.e., annealed at the different temperatures.

Coloration and bleaching were carried out at 1 V and − 0.2 V, respectively, for a duration of 30 s. Figure 5 shows the transmittance data of the films and the values measured

at the middle of the visible spectrum, i.e., 550 nm. EN-100 shows a maximum transmittance of 96.4% in the bleached state and 21.2% in the colored state. This difference (between the colored and bleached states) is defined as the transmittance modulation (ΔT) and is given by:

$$\Delta T = \left(T_b - T_c\right)_\lambda \quad (5)$$

where T_b and T_c are the transmittance in the bleached and colored state, respectively, and λ is the wavelength at which the modulation is measured (i.e., 550 nm). the values being set out in Table I. The transmittance modulation was found to decrease with the increase in annealing temperature, with EN-100 having the highest transmittance modulation of 75.2% and EN-300 with the lowest at 55.6%. Another related parameter to measure the change from the colored to the bleached state is the change in the optical density (ΔOD)[35,44]:

$$\Delta OD = \ln\left(T_b/T_c\right)_\lambda \quad (6)$$

The ΔOD values are set out in Table II, and the highest value is for the EN-100 film. The optical density value is used to calculate the coloration efficiency (η). This is defined
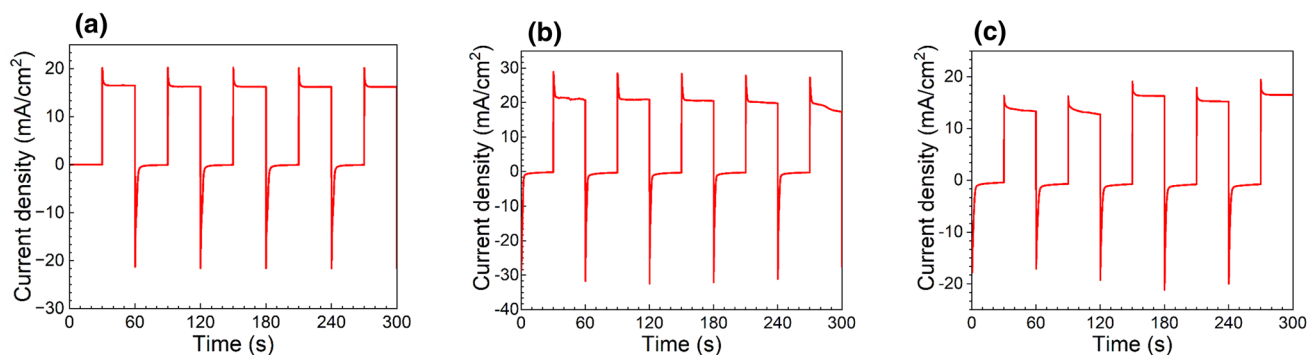

Fig. 3 Chronoamperometry curves of the oxidized NiO films: (a) EN-100, (b) EN-200, and (c) EN-300.

Table I Comparison of various NiO-based EC devices from the literature with the present work

Deposition method of NiO	t_c (s)	t_b (s)	ΔT (%)	η (cm^2/C)	Reference
Plasma-assisted ALD	1.8	1.48	21	118	40
Electrochemical deposition	5.62	4.31	28.8	13.6	41
Spin coating	5.4	3.6	40.1	43.5	42
Hydrolysis	3.92	3.43	78.5	51.8	18
Hydrothermal synthesis	2.0	2.5	77	49	20
Sol–gel dip coating	5.6	2.3	68	-	36
Sol–gel spin coating	3.0	8	59.8	33.6	43
Electroless deposition	3.1	14.1	64.3	12	25
Electroless deposition (EN-100)	1.7	2.8	75.2	20.2	This work
Electroless deposition (EN-200)	2.1	2.0	66.14	13.4	This work
Electroless deposition (EN-300)	2.9	2.6	55.6	12.0	This work

Fig. 4 Images of the EN-100 film in the (a) transparent (bleached) state and (b) colored state; this color change is reversible and occurs upon application of an external potential.
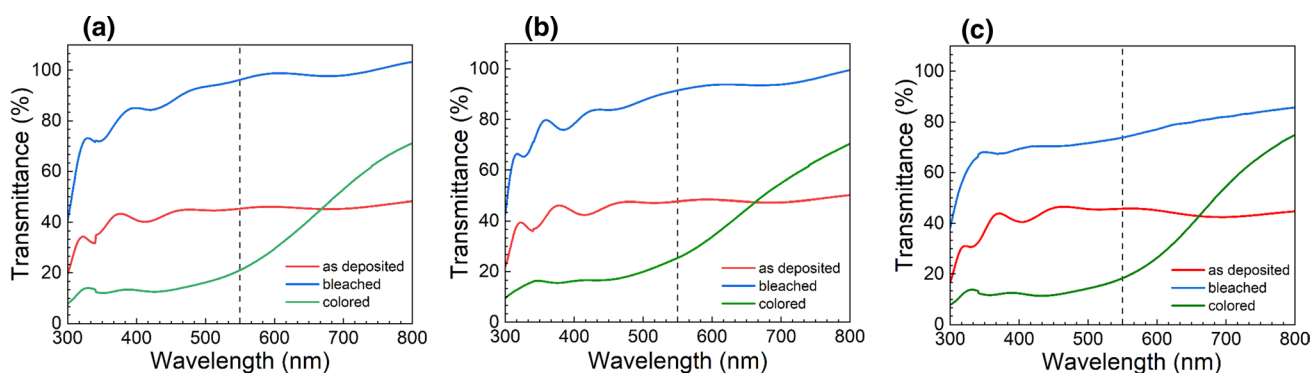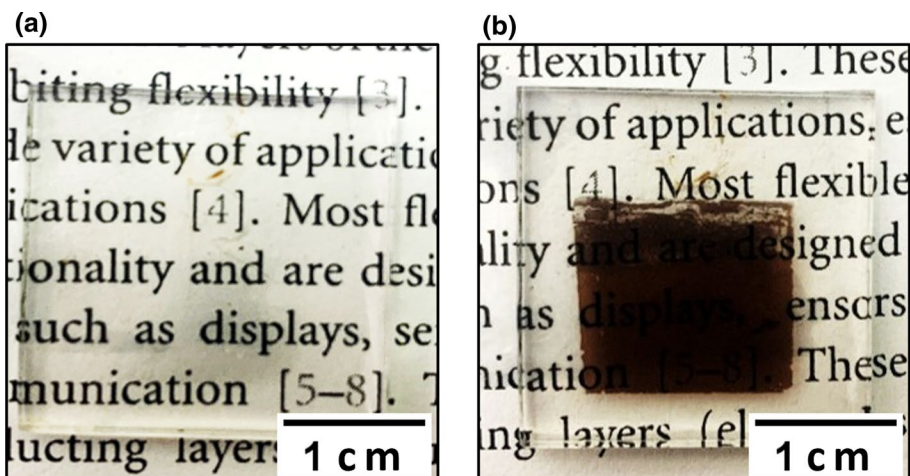

Fig. 5 UV-Vis transmittance spectra showing the transmittance in the as-deposited, colored, and bleached states for (a) EN-100, (b) EN-200, and (c) EN-300; the *vertical dotted line* is drawn at 550 nm to obtain the transmittance values for calculation of the EC properties. The as-deposited transmittance curve is the same for all the samples since this represents the starting Ni film.

Table II Comparison of EC parameters of the EN films

Sample	ΔOD	Q_c (mC/cm^2)
EN-100	0.66	32.6
EN-200	0.56	41.5
EN-300	0.60	50.6

as the ratio of the change in optical density at a specific wavelength to the injected/ejected electronic charge (Q_I), and given by[33,45]:

$$\eta = \left(\frac{OD}{Q_i} \right)_{\lambda=550nm} = \frac{\ln\left(T_b / T_c \right)}{Q_i} \qquad (7)$$

where Q_I is calculated using:

$$Q_i = \int_{t_1}^{t_2} j \, dt \qquad (8)$$

where j is the current density, t_1 and t_2 are the starting and ending times, respectively, of the coloration or bleaching process. The current density, j, and the coloration and bleaching times, t_1 and t_2, are calculated from the CA curves along with the cathodic and anodic charge densities (Q_c and Q_a) which are obtained by calculating the area under the CA curves. The calculated values for the films annealed at different temperatures are compiled in Tables I and II.

From the tables, it can be seen that EN-100 gives the maximum coloration efficiency of 20.2 cm^2/C and that the efficiency decreases with the increasing film annealing temperature. This decrease can be attributed to the decrease in the optical density and, at the same time, the increased charge density requirement for films annealed at higher temperatures.

The data obtained in this work can be compared to the literature values shown in Table I, including our previous work on as-deposited EN films.[25] From both the tables, it can be seen that EN-100 has a better performance in terms of response time, transmittance modulation, and efficiency. The porous morphology of the film due to electrochemical oxidation provides a larger surface area, which helps in faster ion diffusion compared with the other deposition techniques.

This helps the film to have a faster switching between the colored and bleached states compared to films prepared by other techniques.

Electrochromic Solid-State Display Device

The EN-100 film, due to its optimum performance, was further used as an anode to fabricate a solid-state EC display. A display of 2.5 cm × 2 cm size was fabricated by sandwiching PVA/H_3PO_4 polymer gel electrolyte between WO_3 and NiO electrodes. The cyclic voltammetry curve for the device is shown in Fig. 6a. WO_3 shows cathodic coloring behavior, which means that it reversibly changes from colorless to blue color. This color change is due to electron insertion, which changes the oxidation state of tungsten from W^{6+} to W^{5+}.[27] The involved redox equations for the EC behavior are:

$$Cathodic : WO_3(bleached) + x(H^+ + e^-) \rightleftharpoons H_xWO_3(colored)$$
(9)

$$Anodic : H_xNiO(colored) + y(H^+ + e^-) \rightleftharpoons H_{x-y}NiO(bleached)$$
(10)

The response time and the efficiency of the device were evaluated using CA curves, which were obtained by applying potentials of − 3 V (coloration) and 1 V (bleaching) for 30 s each until 300 s (Fig. 6b). The bleaching and coloration times were ~ 4.2 and ~ 3.9 s, respectively. The longer switching time for the device compared to the EN-100 films can be attributed to the frustrated diffusion in the solid gel electrolyte compared to diffusion in the liquid electrolyte. The transition between the deep blue-colored and transparent states at − 3 V and 1 V, respectively, of the EC device are shown in Fig. 7a. These states represent the EC behavior of the solid-state device.

The coloring and bleaching of the device under negative and positive voltages, respectively, can be attributed to the higher complementary charge capacity ratio, which depends on the thickness of the EC films.[46] The complementary charge capacity ratio is the ratio of the surface charge capacity of WO_3 during the insertion of electrons to the surface charge capacity of NiO during the extraction. Hence, the coloration of WO_3 is more prominent due to its greater thickness, while high transparency is maintained during
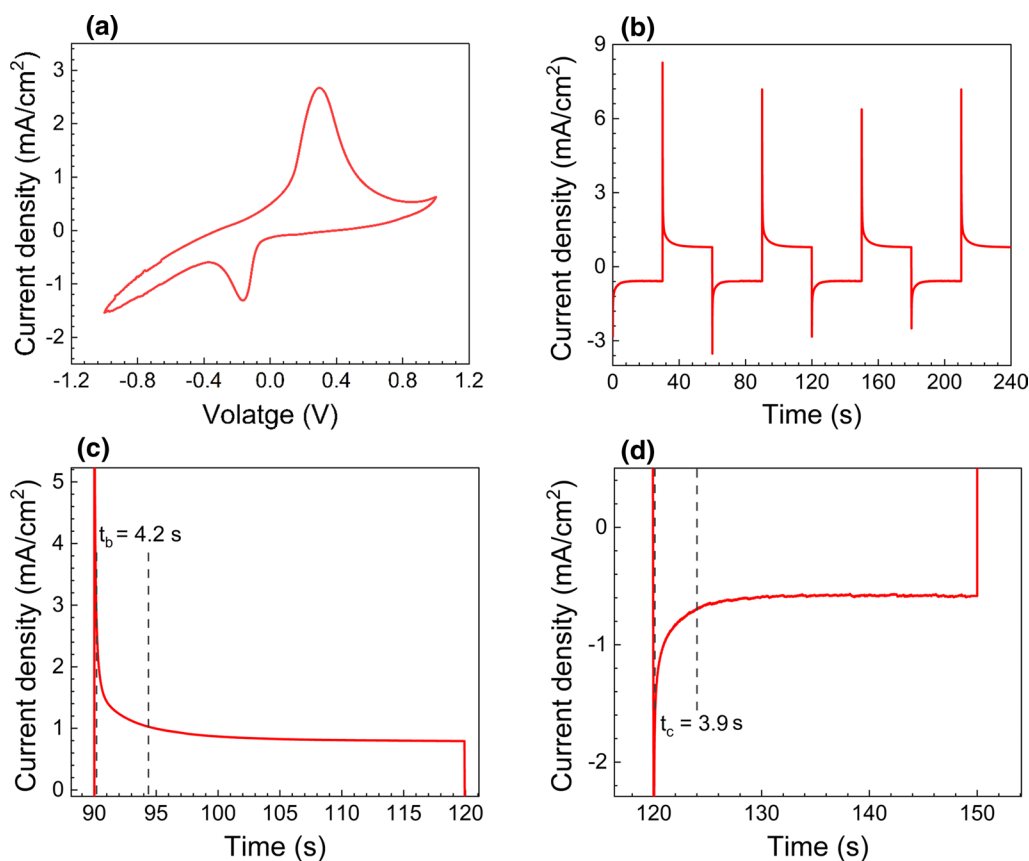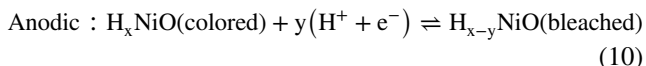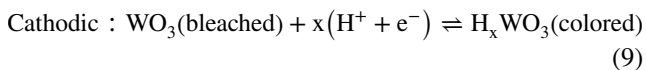

Fig. 6 (a) Cyclic voltammograms of the device recorded in 1.18 M PVA/H_3PO_4 polymer gel electrolyte at a scan rate of 20 mV/s, showing anodic and cathodic peaks at 0.3 and − 0.16 V, respectively; (b) CA curves of the device subjected to potentials of − 3 and 1 V; (c) bleaching and (d) coloration times of the device.
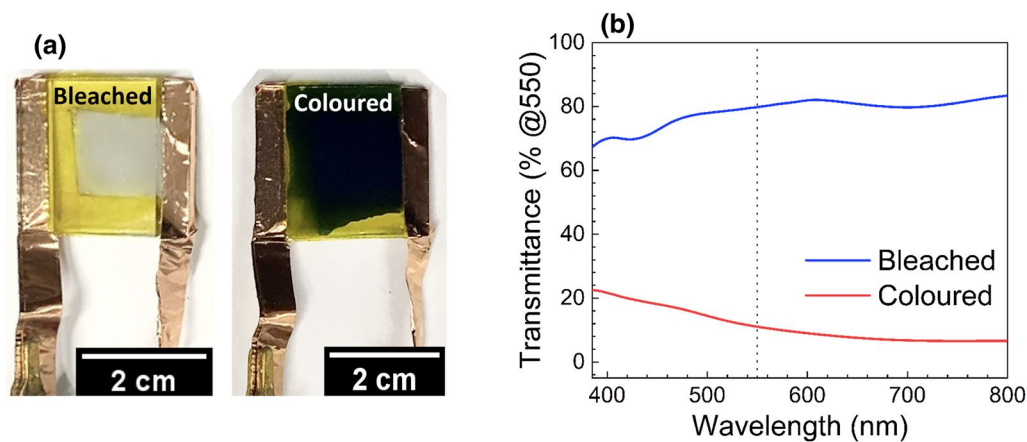
Fig. 7 (a) Images and (b) transmittance spectra of the EC device in bleached (1 V) and colored (− 3 V) states; the deep blue color represents the oxidation of WO_3 at a negative applied voltage.

Table III Comparison of various NiO/WO_3 based EC devices from the literature with the present work

t_c (s)	t_b (s)	ΔT (%)	η (cm²/C)	Ref.
3.1	4.6	46	90	46
10	20	55	87	47
7.9	2.8	–	109.6	48
10	13	75.4	131.9	49
10	11.7	84	55.2	50
3.9	4.2	69	47.3	This work

bleaching due to the lower thickness of the NiO film. Figure 7b shows the UV-visible transmittance of the colored and bleached states of the fabricated device. The transmittance of the colored (T_c) and bleached states (T_b) of the device at 550 nm are 10.9% and 79.9%, respectively, from which ΔT was obtained at 69.0% and the optical density was 0.87 at 550 nm. From the CA curve of the device, Q_c is 18.3 mC/cm². From Eq. (7), the efficiency of the device is calculated to be 47.3 cm²/C. The properties of the fabricated device were comparable to other devices reported in the literature, as seen in Table III.

This EC device can be successfully applied in various applications, such as smart windows, color displays, and sensors. Its applicability can also be extended to smart wearable and flexible electronic devices by utilizing flexible substrates for the deposition of the WO_3 and NiO films.

Conclusions

Uniform NiO films were prepared on FTO substrates using electroless nickel deposition, with different annealing temperatures, followed by electrochemical oxidation in a 1-M KOH bath. Surface morphology studies revealed that the granular morphology of the as-deposited film was changed into a porous structure on electrochemical oxidation. The film annealed at 100°C was found to give superior EC and optical properties with a high transmittance modulation of 75.2%. It also exhibited the fastest response times with 1.7 s and 2.8 s as the coloration and bleaching times, respectively. The efficiency of the EN-100 film was calculated to be 20.2 cm²/C. The fabrication of an electrochromic device was demonstrated using an EN-100 NiO film as the counter electrode. The good performance of the NiO film annealed at low temperature provides a promising route to use this technique to develop flexible EC devices.

Author Contributions M.M.S. designed the experiments, deposited and characterized the NiO films, and drafted the manuscript. N.S. assisted in writing of the manuscript. M.M.S., N.S., and A.M.K. fabricated and characterized the EC device. F.A helped in the deposition and characterisation of the films. A.M.K and S.A. deposited the WO_3 films. P.S. supervised and coordinated this study and revised the manuscript.

References

1. N.M. Nair, M.M. Jahanara, D. Ray, and P. Swaminathan, Photoresponse of a printed transparent silver nanowire-zinc oxide nanocomposite. *Flex. Print. Electron.* 6, 045004 (2021).

2. A. Wibowo, M.A. Marsudi, M.I. Amal, M.B. Ananda, R. Stephanie, H. Ardy, and L.J. Diguna, ZnO nanostructured materials for emerging solar cell applications. *RSC Adv.* 10, 1042838 (2020).

3. M.M. Solly, N. Sharma, and P. Swaminathan, A transparent photodetector based on a composite of silver and tungsten oxide nanowires. *IEEE J. Flex. Electron.* 2, 421 (2023).

4. N. Sharma, N.M. Nair, G. Nagasarvari, D. Ray, and P. Swaminathan, A review of silver nanowire-based composites for flexible electronic applications. *Flex. Print. Electron.* 7, 014009 (2021).

5. J. Ma, Y. Li, J. Li, X. Yang, Y. Ren, A.A. Alghamdi, G. Song, K. Yuan, and Y. Deng, Rationally designed dual-mesoporous transition metal oxides/noble metal nanocomposites for fabrication of gas sensors in real-time detection of 3-hydroxy-2-butanone biomarker. *Adv. Funct. Mater.* 32, 2107439 (2022).

6. R.A. Patil, R.S. Devan, J.-H. Lin, Y.-R. Ma, P.S. Patil, and Y. Liou, Efficient electrochromic properties of high-density and large-area arrays of one- dimensional NiO nanorods. *Sol. Energy Mater. Sol. Cells* 112, 91 (2013).

7. C.G. Granqvist, E. Avendano, and A. Azens, Electrochromic coatings and devices: survey of some recent advances. *Thin Solid Films* 442, 201 (2003).

8. S. Heusing and M. Aegerter, in *Sol-Gel Processing for Conventional and Alternative Energy*. Advances in Sol-Gel Derived Materials and Technologies, ed. by M. Aparicio, A. Jitianu, L. Klein (Springer, Boston, 2012) p. 239.

9. M.Z. Sialvi, R.J. Mortimer, G.D. Wilcox, A.M. Teridi, T.S. Varley, K.U. Wijayantha, and C.A. Kirk, Electrochromic and colorimetric properties of nickel (II) oxide thin films prepared by aerosol-assisted chemical vapor deposition. *ACS Appl. Mater. Interfaces* 5, 5675 (2013).

10. C.G. Granqvist, M.A. Arvizu, I.B. Pehlivan, H.Y. Qu, R.T. Wen, and G.A. Niklasson, Electrochromic materials and devices for energy efficiency and human comfort in buildings: a critical review. *Electrochim. Acta* 259, 1170 (2019).

11. R.I. Eglitis, J. Purans, A.I. Popov, D. Bocharov, A. Chekhovska, and R. Jia, Ab initio computations of O and AO as well as ReO_2, WO_2 and BO_2-terminated ReO_3, WO_3, $BaTiO_3$, $SrTiO_3$ and $BaZrO_3$ (001) surfaces. *Symmetry* 14, 1050 (2022).

12. M. Khairy and S.A. El-Safty, Mesoporous NiO nanoarchitectures for electro-chemical energy storage: influence of size, porosity, and morphology. *RSC Adv.* 3, 23801 (2013).

13. K. Usha, R. Sivakumar, C. Sanjeeviraja, V. Sathe, V. Ganesan, and T. Wang, Improved electrochromic performance of a radio frequency magnetron sputtered NiO thin film with high optical switching speed. *RSC Adv.* 6, 79668 (2016).

14. H. Chen, H. Ma, H. Xia, Y. Chen, and L. Zhang, Optimization parameters of NiO films by dc magnetron sputtering and improvement of electrochromic properties by a mixed electrolyte. *Opt. Mater.* 122, 111639 (2021).

15. H. Lin, Z. Wang, Q. Han, R. Wang, L. Pan, H. Zhu, M. Wan, and Y. Mai, The growth, properties and application of reactively sputtered nickel oxide thin films in all thin film electrochromic devices. *Mater. Sci. Eng. B* 270, 115196 (2021).

16. D. Sahu, T.-J. Wu, S.-C. Wang, and J.-L. Huang, Electrochromic behavior of NiO film prepared by e-beam evaporation. *J. Sci.: Adv. Mater. Devices* 2, 225 (2017).

17. I. Porqueras and E. Bertran, Electrochromic behaviour of nickel oxide thin films deposited by thermal evaporation. *Thin Solid Films* 398, 41 (2001).

18. Y. Tian, Z. Li, S. Dou, X. Zhang, J. Zhang, L. Zhang, L. Wang, X. Zhao, and Y. Li, Facile preparation of aligned NiO nanotube arrays for electrochromic application. *Surf. Coat. Technol.* 337, 63 (2018).

19. E.O. Zayim, I. Turhan, F. Tepehan, and N. Ozer, Sol–gel deposited nickel oxide films for electrochromic applications. *Sol. Energy Mater. Sol. Cells* 92, 164 (2008).

20. F. Cao, G. Pan, X. Xia, P. Tang, and H. Chen, Hydrothermal-synthesized mesoporous nickel oxide nanowall arrays with enhanced electrochromic application. *Electrochim. Acta* 111, 86 (2013).

21. D. Zhou, D. Xie, X. Xia, X. Wang, C. Gu, and J. Tu, All-solid-state electrochromic devices based on WO_3/NiO films: material developments and future applications. *Sci. China Chem.* 60, 3 (2017).

22. J. Wang, X. Huo, M. Guo, and M. Zhang, A review of NiO-based electrochromic energy storage bifunctional material and integrated device. *J. Energy Storage* 47, 103597 (2022).

23. M. Narayanan, A. Harsha, A. Chakraborty, and P. Swaminathan, Reactive bilayers by self-activated electroless nickel-phosphorous deposition on pure aluminum. *JOM* 73, 574 (2021).

24. S. Kundu, S.K. Das, and P. Sahoo, Properties of electroless nickel at elevated temperature-a review. *Procedia Eng.* 97, 1698 (2014).

25. F. Ali, L. Neelakantan, and P. Swaminathan, Electrochromic displays via the room-temperature electrochemical oxidation of nickel. *ACS Omega* 7, 39090 (2022).

26. A. Chakraborty, N.M. Nair, A. Adekar, and P. Swaminathan, Templated electroless nickel deposition for patterning applications. *Surf. Coat. Technol.* 370, 106 (2019).

27. S. Arumugam, A.M. Koshy, F. Ali, P. Swaminathan, M.M. Solly, Magnetron sputtered tungsten oxide films for electrochromic applications, IEEE International Conference on Emerging Electronics IEEE (2022) pp. 1–5. https://doi.org/10.1109/ICEE56203.2022.10117780

28. W. Wang, Z. Li, Z. Yu, and G. Su, The stabilization of $Ni(OH)_2$ by In_2O_3 rods and the electrochromic performance of $Ni(OH)_2$/In_2O_3-rod composite porous film. *Thin Solid Films* 734, 138839 (2021).

29. X. Guo, X. Diao, and W. Wang, Pseudocapacitive contributions to electrochemical kinetics in NiO_x electrochromic anodes. *Ceram. Int.* 47, 22240 (2021).

30. D. Dalavi, M. Suryavanshi, D. Patil, S. Mali, A. Moholkar, S. Kalagi, S. Vanalkar, S. Kang, J. Kim, and P. Patil, Nanoporous nickel oxide thin films and its improved electrochromic performance: effect of thickness. *Appl. Surf. Sci.* 257, 2647 (2011).

31. E. Avendano, H. Rensmo, A. Azens, A. Sandell, G.D.M. Azevedo, H. Siegbahn, G.A. Niklasson, and C.G. Granqvist, Coloration mechanism in proton-intercalated electrochromic hydrated NiO_y and $Ni_{1-x}V_xO_y$ thin films. *J. Electrochem. Soc.* 156, P132 (2009).

32. D.S. Dalavi, R.S. Devan, R.S. Patil, Y.-R. Ma, and P.S. Patil, Electrochromic performance of sol–gel deposited NiO thin film. *Mater. Lett.* 90, 60 (2013).

33. X. Xia, J. Tu, J. Zhang, X. Wang, W. Zhang, and H. Huang, Morphology effect on the electrochromic and electrochemical performances of NiO thin films. *Electrochim. Acta* 53, 5721 (2008).

34. M.-S. Wu and C.-H. Yang, Electrochromic properties of inter-crossing nickel oxide nanoflakes synthesized by electrochemically anodic deposition. *Appl. Phys. Lett.* 91, 033109 (2007).

35. Y. Firat and A. Peksoz, Efficiency enhancement of electrochromic performance in NiO thin film via cu doping for energy-saving potential. *Electrochim. Acta* 295, 645 (2019).

36. K. Purushothaman and G. Muralidharan, The effect of annealing temperature on the electrochromic properties of nanostructured NiO films. *Sol. Energy Mater. Sol. Cells* 93, 1195 (2009).

37. R. Goel, R. Jha, and C. Ravikant, Investigating the structural, electrochemical, and optical properties of p-type spherical nickel

oxide (NiO) nanoparticles. *J. Phys. Chem. Solids* 144, 109488 (2020).

38. A. Ottmann, G. Zakharova, B. Ehrstein, and R. Klingeler, Electrochemical performance of single crystal belt-like $NH_4V_3O_8$ as cathode material for lithium-ion batteries. *Electrochim. Acta* 174, 682 (2015).

39. Y. Wu, G. Wu, X. Ni, and X. Wu, Ion transport in electrochromic nickel oxide thin films. *Sol. Energy Mater. Sol. Cells* 63, 217 (2000).

40. S. Kandpal, I. Ezhov, M. Tanwar, D. Nazarov, D. Olkhovskii, L. Filatov, M.Y. Maximov, and R. Kumar, Plasma assisted atomic layer deposition NiO nanofilms for improved hybrid solid state electrochromic device. *Opt. Mater.* 136, 113494 (2023).

41. V.V. Kondalkar, P.B. Patil, R.M. Mane, P.S. Patil, S. Choudhury, and P.N. Bhosal, Electrochromic performance of nickel oxide thin film: synthesis via electrodeposition technique. *Macromol. Symp.* 361, 47 (2016).

42. C. Zhao, C. Chen, F. Du, and J. Wang, Template synthesis of NiO ultrathin nanosheets using polystyrene nanospheres and their electrochromic properties. *RSC Adv.* 5, 38533 (2015).

43. K.H. Kim, M. Kahuku, Y. Abe, M. Kawamura, and T. Kiba, Improved electrochromic performance in nickel oxide thin film by Zn doping. *Int. J. Electrochem. Sci.* 15, 4065 (2020).

44. M. Fabretto, T. Vaithianathan, C. Hall, P. Murphy, P. Innis, J. Mazurkiewicz, and G. Wallace, Colouration efficiency measurements in electrochromic polymers: The importance of charge density. *Electrochem. Commun.* 9, 2032 (2007).

45. C. Zhang, C. Zheng, S. Zhou, Y. Shen, and C. Zuo, Enhanced electrochromic porous cobalt oxides nanowall electrodes: a new way for fast modulation of yellow-brown light. *Mater. Res. Bull.* 89, 204 (2017).

46. P.-W. Chen, C.-T. Chang, T.-F. Ko, S.-C. Hsu, K.-D. Li, and J.-Y. Wu, Fast response of complementary electrochromic device based on WO$_3$/NiO electrodes. *Sci. Rep.* 10, 8430 (2020).

47. J. Zhang, J. Tu, X. Xia, Y. Qiao, and Y. Lu, An all-solid-state electrochromic device based on NiO/WO$_3$ complementary structure and solid hybrid polyelectrolyte. *Sol. Energy Mater. Sol. Cells* 93, 1840 (2009).

48. J. Pan, R. Zheng, Y. Wang, X. Ye, Z. Wan, C. Jia, X. Weng, J. Xie, and L. Deng, A high-performance electrochromic device assembled with hexagonal WO$_3$ and NiO/Pb composite nanosheet electrodes towards energy storage smart window. *Sol. Energy Mater. Sol. Cells* 207, 110337 (2020).

49. G. Cai, P. Darmawan, M. Cui, J. Chen, X. Wang, A.L.-S. Eh, S. Magdassi, and P.S. Lee, Inkjet-printed all solid-state electrochromic devices based on NiO/WO$_3$ nanoparticle complementary electrodes. *Nanoscale* 8, 348 (2016).

50. M. Rakibuddin, M.A. Shinde, and H. Kim, Sol-gel fabrication of NiO and NiO/WO$_3$ based electrochromic device on ITO and flexible substrate. *Ceram. Int.* 46, 8631 (2020).